



OPEN ACCESS

EDITED BY

Roberto Fedele,
Polytechnic University of Milan, Italy

REVIEWED BY

Agus Prasetyo,
National Research and Innovation Agency
(BRIN), Indonesia
Nicola Cefis,
Polytechnic of Milan, Italy

*CORRESPONDENCE

Halima Chaa,
✉ halima.chaa@univ-temouchent.edu.dz

RECEIVED 02 November 2025

REVISED 20 January 2026

ACCEPTED 21 January 2026

PUBLISHED 17 February 2026

CITATION

Chaa H, Krouri Z, Akli O and Allam D (2026)
From quartzose sandstone to metallurgical
grade silicon feedstock for photovoltaics: an
integrated sieving, magnetic separation and
acid leaching protocol.
Front. Mater. 13:1737892.
doi: 10.3389/fmats.2026.1737892

COPYRIGHT

© 2026 Chaa, Krouri, Akli and Allam. This is an
open-access article distributed under the
terms of the [Creative Commons Attribution
License \(CC BY\)](https://creativecommons.org/licenses/by/4.0/). The use, distribution or
reproduction in other forums is permitted,
provided the original author(s) and the
copyright owner(s) are credited and that the
original publication in this journal is cited, in
accordance with accepted academic practice.
No use, distribution or reproduction is
permitted which does not comply with
these terms.

From quartzose sandstone to metallurgical grade silicon feedstock for photovoltaics: an integrated sieving, magnetic separation and acid leaching protocol

Halima Chaa^{1*}, Zohra Krouri², Ouissam Akli² and
Djaouida Allam²

¹University of Belhadj Bouchaib, Ain Témouchent, Algeria, ²Laboratory of Applied Chemistry and Chemical Engineering, University of Mouloud Mammeri, Tizi-Ouzou, Algeria

Finding new sources of high purity silica is becoming increasingly important for solar panel manufacturing. Behind quartz, sandstone can be one of the most important sources of silica for advanced technological applications. Despite its abundance in the Earth's crust, the widespread use of sandstone is limited by the presence of undesirable oxide. This is the case for the studied sandstone rocks, where impurities, particularly iron and aluminum oxide, restrict the suitability of this silica for producing advanced materials. This work presents an optimized multistage purification protocol specifically engineered for quartzose sandstone. We systematically characterize quartzose sandstone from northern Algeria, an abundant yet underexploited sedimentary resource, demonstrating an initial rich silica content but with problematic levels of Fe₂O₃ and Al₂O₃ impurities. The core scientific contribution is the establishment of a tailored sequence: granulometric sieving to isolate the optimal 250–400 μm fraction (89.15% SiO₂), dry high intensity magnetic separation, and optimized acid leaching using 4 M HCl at 90 °C for 2 h that show leaching efficiency plateaus. Mechanical analysis reveals the 250–400 μm fractions as a liberation sweet spot where quartz grains are maximally freed from the detrital matrix. The results are encouraging, demonstrating that the applied process successfully increased the silica content from an average of 89.15%–99.28%. Furthermore, it significantly reduced the impurity levels, lowering the iron oxide content from 0.27% to 0.02% and the alumina content from 2.46% to 0.02%. By demonstrating the viability of sandstone as a photovoltaic grade feedstock precursor for metallurgical grade silicon (MG-Si) production, which is the essential first step in manufacturing solar grade silicon (SoG-Si) for photovoltaics, this work provides a scalable pathway for diversifying the solar industry's silica supply chain.

KEYWORDS

leaching, magnetic separation, photovoltaic, sandstone, sieving, silica, washing

1 Introduction

High purity quartz (HPQ), defined as SiO₂ content exceeding 99.9% with stringent limits on deleterious elements like Fe, Al, and Ti, it is a critical raw material for advanced technological applications, most notably the production of solar grade silicon (SoG-Si) for photovoltaics (PV) (Vatalis et al., 2015) (Table 1). Global demand for PV is projected to grow exponentially, intensifying pressure on high purity quartz supply chains, which are currently dominated by a limited number of geological deposits. This concentration reveals strategic and economic risks, driving the urgent need to identify and validate alternative, abundant silica sources (Yu et al., 2025).

Quartzose sandstone represents one of the most voluminous and geographically widespread silica rich sedimentary rocks (BRGM, 2019; Vatalis et al., 2015). Countries with significant sandstone deposits, such as Algeria with its extensive Numidian facies, possess a potential resource for high purity silica production (ASGA, 2015; Chkotov, 1979; Gouski and Ourak, 1986; Hadjem, 2010). However, the industrial utilization of sandstone has been historically limited. Its silica is locked within a detrital structure cemented by various impurity phases predominantly iron oxide, aluminum clays which preclude its direct use in high tech applications (Xie et al., 2023). These impurities, even at trace levels, can severely degrade the performance and efficiency of high grade silica (Braga et al., 2008; Chen et al., 2019).

The established industrial purification of quartz is a multistage process that sequentially combines physical pretreatment, thermal, and chemical methods (Pan et al., 2022; Zhang et al., 2025; Wang et al., 2025), their systematic application and optimization for consolidated sandstone matrices remain unexplored at both pilot and industrial scales. Recent reviews of silica extraction technologies underscore this significant gap: extensive research focuses on quartz veins, sands, and industrial by products, while consolidated sedimentary rocks are consistently overlooked despite their sheer abundance (Pan et al., 2022). Quartz purification often employs aggressive reagents like hydrofluoric acid (HF) to achieve sub 100 ppm Fe levels for SoG-Si, but these methods

entail severe environmental, safety, and waste management challenges (Wang et al., 2018; Xie et al., 2023). Alternative acids like H₂SO₄ or H₃PO₄ show variable efficiency and can introduce secondary precipitation issues (Zhang et al., 2012). More critically, these protocols are designed for granular quartz and fail to address the fundamental challenge in sandstone processing, the requirement for effective mechanical liberation of quartz grains from a cemented, impurity rich matrix prior to chemical purification (Bouabdallah et al., 2015).

This study directly addresses this gap by initiating a comprehensive investigation into the adaptation and optimization of a sequential mechanical and chemical purification process specifically for quartzose sandstone. Our objectives are: (1) to conduct an in depth characterization of the sandstone feedstock, (2) to establish sandstone purification process (sieving, magnetic separation, acid leaching), and (3) to critically evaluate the technical feasibility and purity of the final silica concentrate against international standards for PV applications.

2 Materials and methods

2.1 Geological samples

The raw materials for this study are quartzose sandstone from the Numidian flysch facies in the Kabylia region (Tizi-Ouzou, northern Algeria). This formation is estimated to hold substantial reserves of approximately 16.6 million tons, with favorable mining conditions (Belousov and Ismailov, 1987). For this work, about ten samples were collected from massive sandstone addressing the worst case compositional scenario to ensure the robustness of the purification process across the natural variability of the sandstone. Petrographic analysis was conducted on thin sections using a ZEISS Axio optical microscope at the École Normale Supérieure (ENS), Kouba, Algeria and the morphology of grains was examined using an OPTECH binocular magnifier at the national school of marine sciences and coastal management, Algeria (ENSSMAL).

TABLE 1 Minimum SiO₂ content requirements for each grade of quartz products (Richard Flook).

Type of application	SiO ₂ % (Minimum)	Other elements (Maximum %)
Clear glass grade sand	99.5	0.5
Semiconductors, optical glass, and LCDs	99.8	0.2
Low-grade, high-purity quartz	99.95	0.05
Medium-grade, high-purity quartz	99.99	0.01
High-grade, high-purity quartz	99.997	0.003

Specific requirements may be limited by other applications. For example, Fe₂O₃ < 100 ppm for float glass and Fe₂O₃ < 40 ppm for low-iron float glass.

Typically, "high purity" quartz has Fe₂O₃ < 15 ppm, Al₂O₃ < 300 ppm, and alkaline earth and alkaline earth oxides < 150 ppm.

In some practices, Al₂O₃ can replace some SiO₂, such as up to 1.5% Al₂O₃ in float glass.

Threshold limits may vary depending on the composition of the other raw materials used in the application.

LCD: Liquid crystal display.

"High-grade" high-purity quartz, impurities < 30 ppm, standard high-purity material from Unimin (Iota).

TABLE 2 Results of the granulometric analysis, showing the distribution of particle sizes in the sandstone samples after grinding.

Fraction N°	Grain-size distribution (µm)	Weight (g)	Weight (%)
E ₁	+800 µm	83.41	11,66
E ₂	630–800 µm	7.03	0,98
E ₃	400–630 µm	57.05	7,98
E ₄	250–400 µm	162.11	22,67
E ₅	160–250 µm	220.19	30,79
E ₆	140–160 µm	20.98	2,93
E ₇	100–140 µm	129.76	18,14
E ₈	–100 µm	34.99	4,89

Total Mass = 715.22 g.

2.2 Grinding and granulometric separation

For the sandstone enrichment, the initial step involved crushing, grinding, and granulometric sieving of the rock. This protocol was adapted from the method established by Huang et al. (2013) for quartz minerals.

For initial bulk chemical characterization, a 50 g split was pulverized to a fine powder (<100 µm) in an agate mortar. For the granulometric study, the sandstone samples was ground using a planetary ball mill (Pulverisette mono, Fritsch) equipped with an agate grinding jar and balls, milling was conducted at 200 rpm for 20 min. The resulting product (715.22 g) was sieved for 15 min using a mechanical shaker (Retsch AS 200) and a stack of standard ASTM sieves with apertures of 800, 630, 400, 250, 160, 140, and 100 µm.

The granulometric sieving of the sandstone quartz grains yielded size fractions ranging from +800 µm to –100 µm, with the following classes: +800 µm, 630–800 µm, 400–630 µm, 250–400 µm, 160–250 µm, 140–160 µm, 100–140 µm, and –100 µm (Table 2). Subsequently, each separated grain size fraction underwent chemical testing by XRF to evaluate its composition. The objective of this analysis was to determine whether the different particle size groups contained similar concentrations of silica.

2.3 Chemical and mineralogical characterization

Bulk chemical composition of each granulometric fraction was determined using a Rigaku wavelength dispersive XRF spectrometer at the research center of physico-chemical analysis (CRAPC), Bousmail, Algeria. Analytical accuracy for major oxide (SiO₂, Al₂O₃, Fe₂O₃) is ±0.5% (relative), with typical detection limits of 0.01% (100 ppm).

High resolution microanalysis were performed at CRTSE research center, Algeria, using a JEOL JXA-8230 SuperProbe Electron Probe Micro-Analyzer (EPMA) equipped with five wavelength-dispersive spectrometers (WDS), operating at 15 kV and 20 nA.

Mineral phase identification was performed using X-ray Diffraction of a PANalytical X'Pert Pro diffractometer at the research center for studies and technical services for the construction materials industry (CETIM), Boumerdes, Algeria. Measurements were taken with Cu-Kα radiation ($\lambda = 1.5406 \text{ \AA}$) over a 2θ range of 5°–70°.

2.4 Mechanical treatment: magnetic separation and washing

Based on XRF results, the 250–400 µm fraction (162.11 g), which exhibited the highest natural SiO₂ content, was selected for purification by magnetic separation, this fraction was processed using a CARPCO laboratory scale induced roll magnetic separator in National office of geological and mining research, ORGM, Boumerdès. Key operating parameters were: magnetic flux density = 1.6 T, applied current = 10 A, feed rate = controlled via vibrating feeder, roll rotation speed = 60 rpm.

The magnetically treated sand (100 g) was then subjected to an attrition washing step. The material was placed in 500 mL of distilled water, stirred vigorously for 10 min to dislodge loosely adhered fines and clays, and subsequently passed over an 80 µm sieve. The retained solids were rinsed thoroughly with distilled water and dried in an oven at 70 °C for 2 h.

2.5 Chemical leaching: experimental design and procedure

The dissolution of impurity oxides (Fe₂O₃, Al₂O₃) using HCl lixiviant is governed by a surface reaction mechanism, where protons attack the metal oxygen bonds. For iron oxide, the reaction $\text{Fe}_2\text{O}_3(\text{s}) + 6\text{H}^+(\text{aq}) \rightarrow 2\text{Fe}^{3+}(\text{aq}) + 3\text{H}_2\text{O}$ is facilitated by the formation of soluble chloro-complexes, which shift the equilibrium toward dissolution (Dvoretzkii et al., 2002; Nouioua and Barkat, 2017). Aluminum oxide dissolves via a similar protonation



FIGURE 1
Macroscopic view of the studied quartzose sandstone sample.

pathway, though their kinetics is often slower due to a more stable passivation layer.

Acid leaching was optimized using hydrochloric acid (HCl, 37% analytical grade). A full factorial design tested four HCl concentrations: 2 M, 3 M, 4 M, and 5 M. Each experimental condition was performed to ensure reliability. For a single leaching experiment, the following protocol was strictly adhered to:

- Solid charge: Precisely 25.00 g (± 0.05 g) of the pretreated (magnetically separated and washed) sandstone.
- Leaching solution: 200 mL of the specified HCl concentration, giving a constant solid to liquid (S/L) ratio of 1:8 (w/v). Leaching was conducted in a 500 mL Erlenmeyer flask placed on a temperature controlled hotplate with magnetic stirring (800 rpm). A reflux condenser was attached to prevent solvent evaporation. The slurry was heated to and maintained at $90 \text{ }^\circ\text{C} \pm 2 \text{ }^\circ\text{C}$ for 2 h.
- Post treatment: The slurry was immediately vacuum filtered. The solid residue was washed with 500 mL of distilled water to neutral pH and dried at $70 \text{ }^\circ\text{C}$ for 2 h. The mass of the final product was recorded. The spent acid leachate was collected and neutralized to pH 7.0 using a 10% NaOH solution prior to disposal, following standard laboratory safety and environmental protocols. The final leached products from all conditions were characterized by XRF.

3 Result

3.1 Quartzose sandstone characterization before treatment (raw materials)

3.1.1 Macroscopic study

A macroscopic study of the siliceous sandstone reveals a massive, very hard rock with a grayish hue (Figure 1). The rock's constituent grains are small and visible to the naked eye, being primarily composed of vitreous quartz alongside occasional reddish colored iron oxide minerals (Chaa et al., 2025).

The studied sandstone possesses favorable physical properties for processing: bulk density of 2.4 g/cm^3 , porosity 7.34%–14.06%, and considerable mechanical strength (dry compressive strength of 1050 kg/cm^2) (Abed and Hakem, 2017).

3.1.2 Microscopic study

Microscopic observation of the sandstone thin sections confirmed that quartz is the primary mineral constituent, dominating the overall composition. The analysis also revealed notable inclusions, such as oxidized biotite (Figure 2a) and iron oxide (Figure 2b), which are occasionally present within the quartz grains themselves. Accessory minerals, including muscovite, pyrite and zircon, were also identified in minor quantities; the presence of mineral impurities necessitates a refinement process (Kheloufi et al., 2013; Kefai et al., 2020).

3.1.3 Chemical and mineralogical characterization

The X-ray diffraction (XRD) pattern of the analyzed siliceous sandstone showed distinct diffraction peaks at characteristic 2θ positions, including 20.9° , 26.6° , 36.5° , 39.4° , 42.5° , 50.1° , and 59.9° (Figure 3). These peaks correspond to the crystallographic planes of quartz, confirming its high crystallinity. This high crystallinity underscores the material's potential for solar industrial applications (Désindes, 2005). The intensity of these peaks, particularly the prominent one at 26.6° , indicates a significant abundance of quartz.

To characterize the raw sandstone material used in this study and confirm its suitability for the silicon metallurgy industry, Electron Probe Micro-Analyzer (EPMA) was utilized for high resolution, spatially resolved quantification of elemental distributions, ensuring the detection of trace impurities critical for solar energy sector (Götze and Möckel, 2012).

The EPMA analyses confirmed that the sandstone is predominantly rich in silica, elemental mapping clearly shows that Al is more diffusely distributed, corresponding to the clay rich cement (Figure 4), with minor impurities including Fe, Ca, K, as illustrated in the EPMA profiles (Figure 5). Critically, no boron (B)

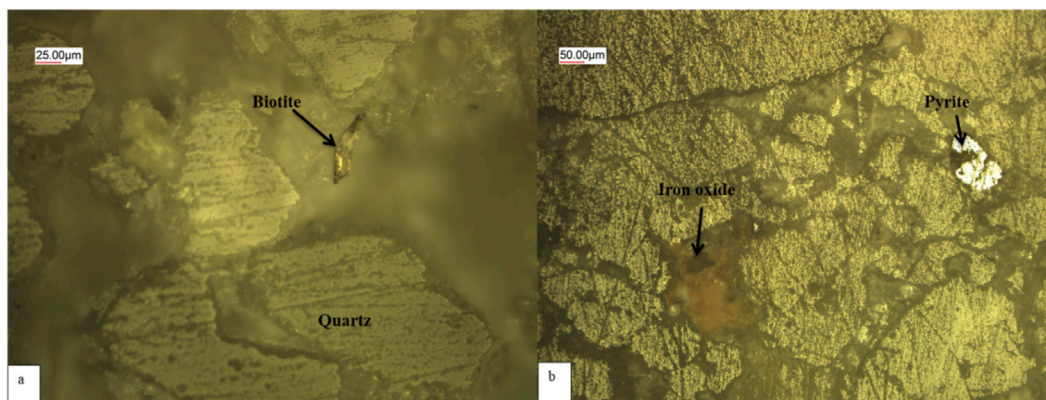


FIGURE 2 Microscopic observation (a) Sandstone with micas (biotite), (b) sandstone with oxide.

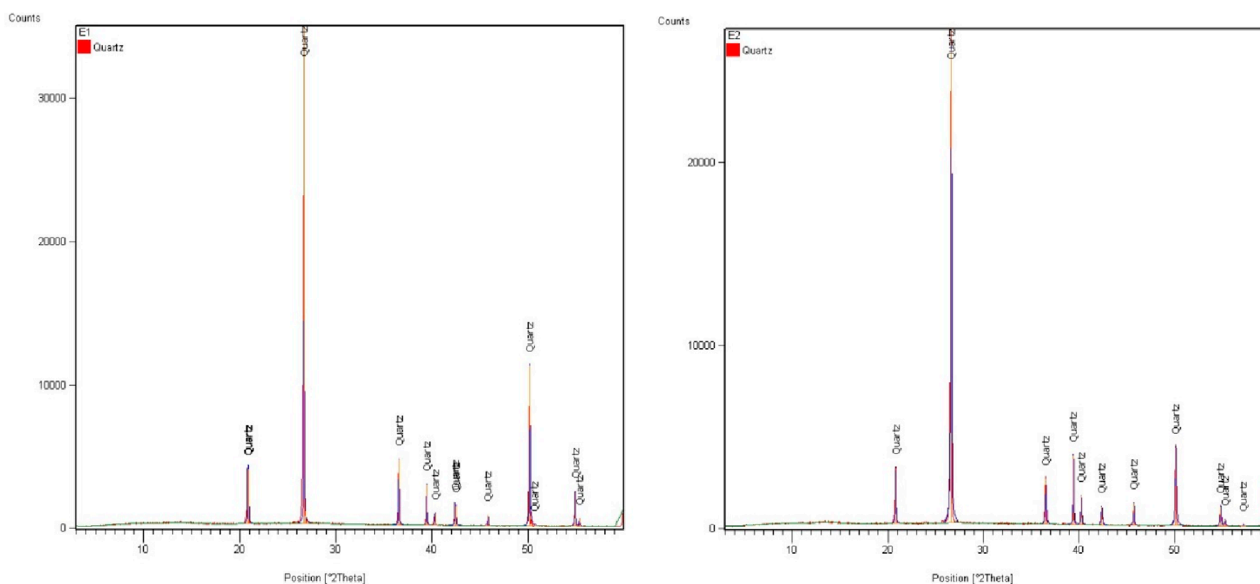


FIGURE 3 X-ray diffraction (XRD) pattern of the raw quartzose sandstone.

was detected above the EPMA detection limit (0.3%), a favorable characteristic for PV feedstock (Chen et al., 2019).

3.2 Sandstone's treatment and their characterization

3.2.1 Granulometric analysis

The analysis revealed that the 250–400 µm fraction possessed the highest silica content of 89.15%, along with the lowest levels of impurities, notably 0.27% Fe_2O_3 and 2.46% Al_2O_3 . Other minor impurities are listed in Table 3. Consequently, the 250–400 µm fraction was selected for further enrichment through magnetic separation, washing, and acid leaching.

The superior purity observed in the 250–400 µm fraction can be explained by the mineral liberation characteristics and impurity distribution within the sandstone matrix. Quartz grains which are inherently harder and more resistant to fracture tend to cleave along crystallographic planes, producing particles in this intermediate size range with minimal attached impurities. In contrast, finer fractions (<100 µm) contain a higher proportion of liberated clay minerals, micas, and iron oxide fines, which are preferentially generated from the softer, more friable cementing phases.

Microscopic examination (Figures 2a,b) confirms that iron oxide and aluminosilicate are predominantly located at grain boundaries and within microfractures. The 250–400 µm size range appears to represent an optimal liberation window where quartz grains are sufficiently freed from the cement matrix.

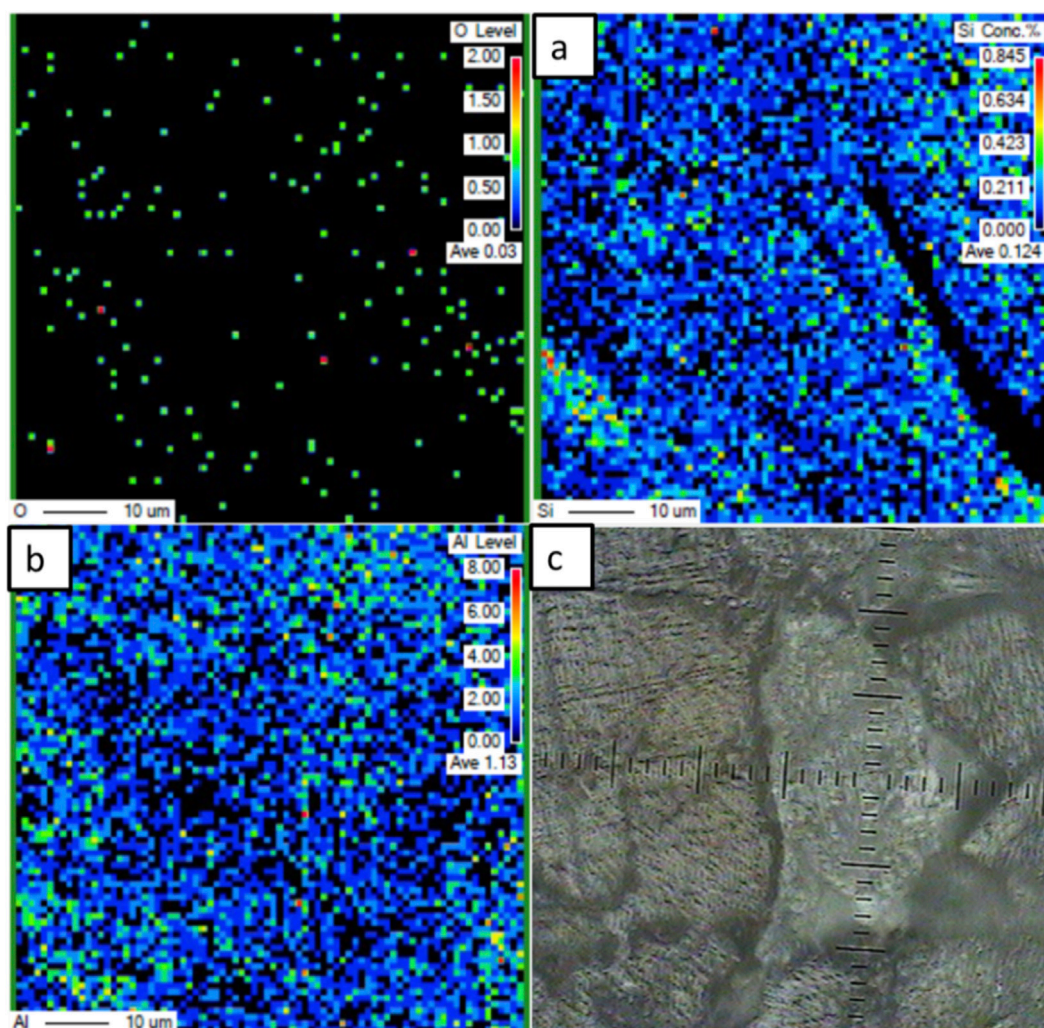


FIGURE 4 Electron Probe Micro-Analyzer (EPMA) elemental mapping of the untreated sandstone sample showing the distribution of (a) silicon (Si, wt%) and (b) aluminum (Al, wt%) within quartz grains (c).

Furthermore, morphological observation using a binocular magnifier on 250–400 µm samples confirms distinct grain characteristics:

Intact quartz grains: These grains displayed a distinct morphology with defined facets and sharp edges, resulting in a vitreous luster. A fine layer of silica powder was often observed adhering to their surfaces (Figure 6a).

Iron oxide: Particles of iron oxide were identified, either adhering to the surfaces of quartz grains or dispersed within the sample.

3.2.2 Magnetic separation

The 250–400 µm fraction was processed using a high intensity, dry magnetic separator to remove the iron inclusions previously identified by microscopic observation and confirmed by XRF analysis. In this process, the sandstone powder was fed via a hopper and a vibrating feeder. The dry magnetic separation of the 250–400 µm sample step attained a 0.14% reduction in Fe₂O₃ (from

0.27% to 0.13%) and a 0.12% reduction in TiO₂ (from 0.36% to 0.24%). This efficiency is attributed to the removal of ferromagnetic and paramagnetic particles. However, the limited removal of non-magnetic iron oxide of hematite and finely disseminated rutile within quartz grains (Figure 5) explains the incomplete purification at this stage.

3.2.3 Washing

The washing step was performed to remove sticky mud, dust, and any remaining ferruginous or clayey incrustations from the quartz grains. A further objective was to evaluate the potential for reducing alumina and other impurities without resorting to acid treatment.

Washing the magnetically separated fraction (250–400 µm) reduced Al₂O₃ content by 0.28% (from 0.87% to 0.59%) and Fe₂O₃ by 0.03% (from 0.13% to 0.10%), alongside an increase in the SiO₂ content by 1% (Table 4).

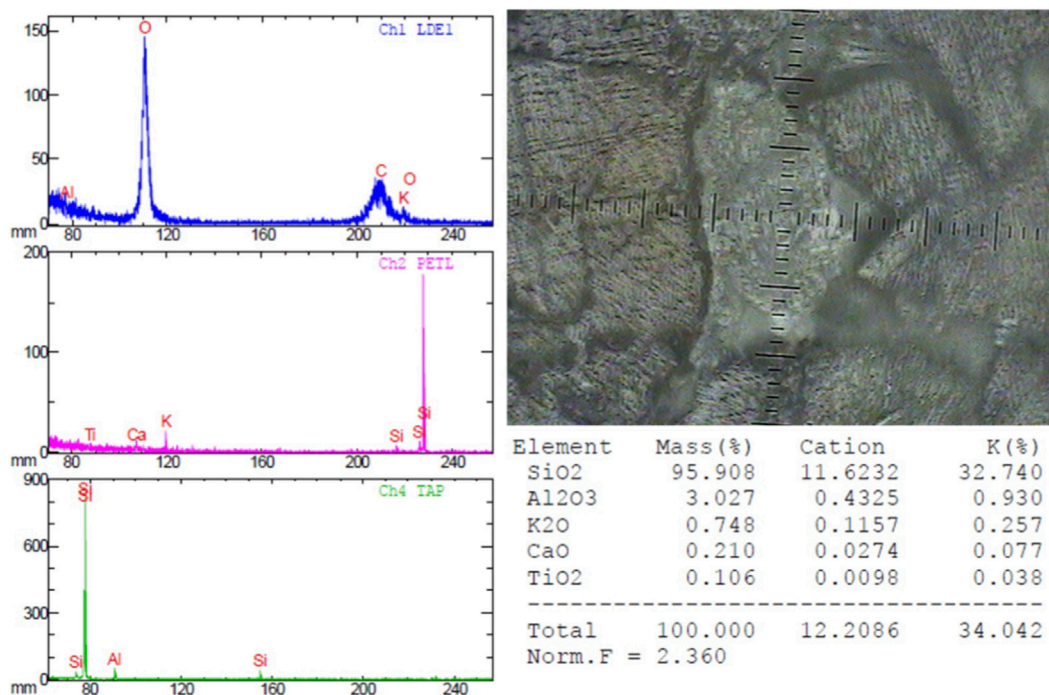


FIGURE 5 EPMA concentration profiles of major elements in the untreated quartzose sandstone showing Al, K, Ca, and Ti disseminated within quartz grains.

TABLE 3 Results of X-ray fluorescence chemical analyses of the particle size fractions of quartzose sandstone.

Fractions size (µm) %	+800	630–800	400–630	250–400	160–250	140–160	100–140	–100
SiO ₂	85.97	79.26	84.81	89.15	86.12	86.12	85.06	85.20
Al ₂ O ₃	3.29	4.25	2.91	2.46	4.31	4.31	3.63	3.86
Fe ₂ O ₃	0.41	0.56	0.27	0.27	0.54	0.54	0.51	0.51
CaO	0.03	0.08	0.07	0.03	0.08	0.08	0.04	0.06
MgO	0.18	0.15	0.12	0.04	0.13	0.13	0.17	0.14
SO ₃	0.02	0.06	0.02	0.02	0.02	0.02	0.01	0.01
K ₂ O	0.48	0.65	0.35	0.30	0.60	0.60	0.59	0.40
Na ₂ O	0.07	0.06	0.03	0.02	0.03	0.03	0.05	0.29
P ₂ O ₅	0.02	0.03	0.02	0.01	0.02	0.02	0.00	0.03
TiO ₂	1.00	0.68	0.37	0.36	0.98	0.98	0.97	1.03
Cr ₂ O ₃	0.08	0.08	0.05	0.04	0.09	0.09	—	0.13
ZnO	—	0.01	0.00	0.02	0.09	0.09	0.04	0.07
ZrO ₂	0.08	0.17	0.06	0.05	0.17	0.17	0.13	0.28
CO ₂	9.29	13.83	10.83	7.12	6.72	6.72	8.69	7.88

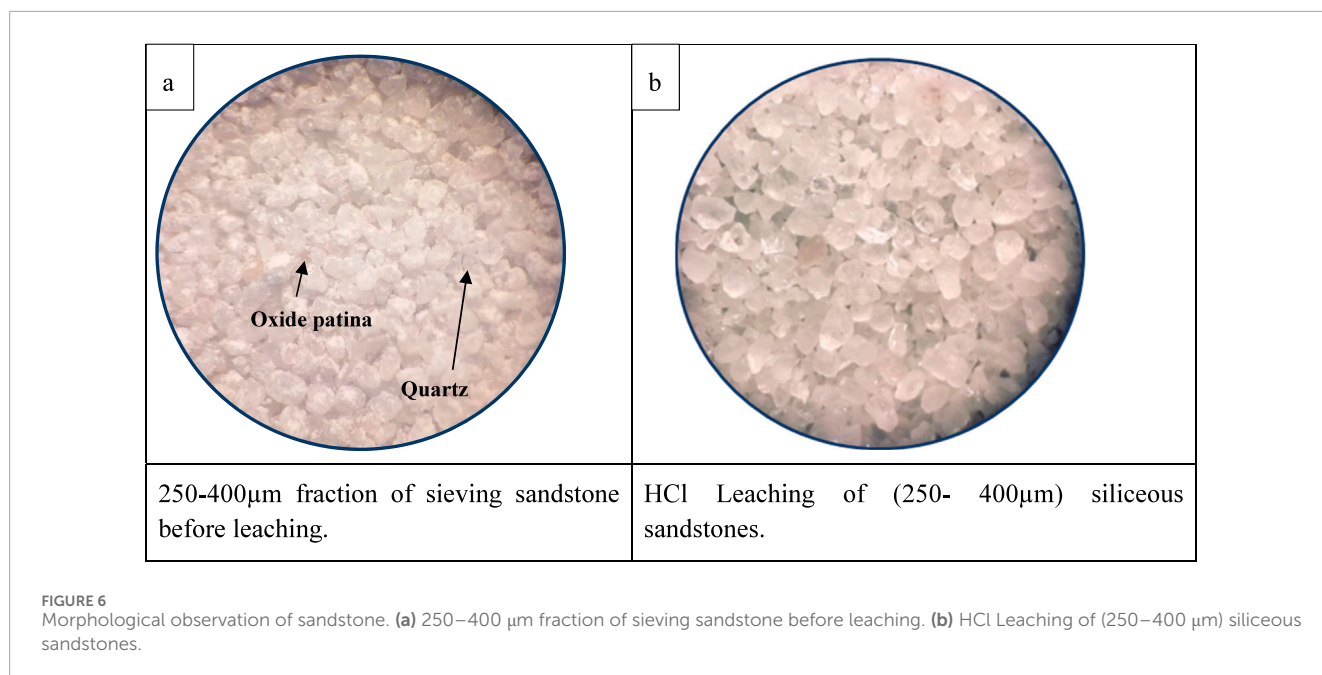


FIGURE 6 Morphological observation of sandstone. (a) 250–400 μm fraction of sieving sandstone before leaching. (b) HCl Leaching of (250–400 μm) siliceous sandstones.

TABLE 4 Results of X-ray fluorescence chemical analyses of quartzose sandstone after enrichment.

Oxide elements	After magnetic separation	After washing	2M HCl + washing	3M HCl + washing	4M HCl + washing	5M HCl + washing
SiO ₂	95.82	96.00	96.85	96.93	99.28	99.13
Al ₂ O ₃	0.87	0.59	0.02	0.45	0.02	0.04
Fe ₂ O ₃	0.13	0.10	0.04	0.11	0.02	0.11
CaO	1.12	1.13	0.11	1.09	0.11	0.14
MgO	0.25	0.23	0.00	0.23	0.00	0.00
SO ₃	0.01	0.01	0.08	0.01	0.08	0.08
K ₂ O	0.12	0.07	0.01	0.04	0.01	0.02
Na ₂ O	0.04	0.03	0.00	0.05	0.00	0.00
P ₂ O ₅	0.04	0.04	0.02	0.03	0.02	0.02
TiO ₂	0.24	0.19	0.05	0.15	0.05	0.05
ZnO	0.03	0.02	0.00	0.02	0.00	0.00
Mn ₂ O ₃	0.07	0.07	0.01	0.08	0.01	0.02
SrO	0.08	0.08	0.01	0.07	0.01	0.01

However, the results confirm that washing alone is insufficient to achieve the desired silica purity level. This is attributed to the persistent presence of oxides that are tightly adhered or percolated onto the quartz grains, a phenomenon previously observed during microscopic examination (Figure 2b). These intergrown impurities require chemical dissolution for complete removal.

3.2.4 Acid leaching

The 250–400 μm fraction was leached following the protocol in Section 2.5, using HCl concentrations of 2, 3, 4, and 5 M.

The results confirmed that acid leaching with HCl significantly reduces impurities in a concentration dependent manner. A marked decrease in metallic components, primarily iron, was observed

TABLE 5 Chemical comparison of raw materials and process product composition.

Oxide elements	Raw materials (%)	Processed product (%)	Ratio (%)
SiO ₂	89.15	99.28	+10.13%
Al ₂ O ₃	2.46	0.02	-2.44%
Fe ₂ O ₃	0.27	0.02	-0.25%
TiO ₂	0.36	0.05	-0.31%
Na ₂ O	0.02	0.00	-0.02%
MgO	0.04	0.00	-0.04%

with increasing HCl concentration. At 2 mol/L, a slight decrease of 0.04% in Fe₂O₃ and 0.02% in Al₂O₃ was achieved. The optimum removal efficiency was observed at 4 mol/L (Figure 6b), achieving a final content of 0.02% for both Fe₂O₃ and Al₂O₃. No significant improvement was observed at a higher concentration of 5 mol/L, which resulted in a slower removal rate.

Consequently, the most effective treatment was identified as 4M HCl. This optimal condition successfully increased the final silica content to 99.28%, while reducing impurity levels to 0.02% Fe₂O₃, 0.02% Al₂O₃, and 0.05% TiO₂ (Table 4).

4 Discussion

Based on the comprehensive dataset, the developed sequential purification protocol of granulometric sieving, magnetic separation, washing, and acid leaching successfully upgrades the quartzose sandstone from 89.15% to 99.28% SiO₂, while reducing Fe₂O₃ and Al₂O₃ to 0.02% each (Table 5). The data reveal that the 250–400 μm fraction represents a critical liberation window, yielding the highest innate purity and optimal response to subsequent treatments, an intermediate particle sizes often represent the optimal balance between mineral liberation and overgrinding (Wills and Finch, 2015). Magnetic separation preferentially removed discrete ferromagnetic impurities but limited removal of non-magnetic iron oxide of hematite and finely disseminated rutile within quartz grains, washing effectively eliminated clay bound alumina. The poor iron reduction during washing further indicates that residual iron and titanium oxide are either occluded within quartz grains. However, 4M HCl leaching dissolved the occluded and chemically bound oxide inaccessible to physical methods. The leaching kinetics indicates a process controlled by surface reaction up to 4M HCl, beyond which diffusion limitations and potential reprecipitation effects explain the observed efficiency plateau.

The selection of hydrochloric acid (HCl) as the leaching agent was based on a comparative analysis of efficiency, cost, and environmental manageability. While hydrofluoric acid (HF) achieves superior iron removal, its use requires 40%–60% higher stoichiometric consumption per unit of dissolved Fe₂O₃ and generates hazardous calcium fluoride sludge (CaF₂), introducing significant waste management burdens (Wang et al., 2018;

Xie et al., 2023). Sulfuric acid (H₂SO₄), on the other hand, often promotes secondary precipitation of metal sulfates that can readsorb onto silica surfaces, impairing final purity (Zhang et al., 2012). In our optimized protocol using the 250–400 μm fraction of pretreated sandstone, leaching with 4 M HCl at 90 °C for 2 h (solid/liquid ratio of 1/8) increased the SiO₂ content from 96.00% to 99.28% (+3.28%), while reducing Al₂O₃ from 0.59% to 0.02% and Fe₂O₃ from 0.10% to 0.02%. The corresponding consumption of concentrated HCl (37%) was approximately 2.4 L per kilogram of treated sand to prepare the required 4 M leaching solution.

The concentrate (99.28% SiO₂, 0.02% Fe₂O₃, 0.02% Al₂O₃, 0.05% TiO₂) exceeds the standard chemical specifications for a feed material in the production of Metallurgical Grade Silicon (MG-Si), which typically requires > 98.5% SiO₂ (Schei, Tuset, and Tveit, 1998) and tolerates Fe and Al levels up to 0.1% and 0.2%, respectively. This position can make the studied material as a chemically alternative to conventional quartz feedstocks for the carbothermic reduction process. Therefore, the process successfully transforms local sandstone into a high value feedstock for MG-Si production, which is the essential first step in the silicon value chain for photovoltaics. The principal challenge for industrial adoption is no longer chemical purity for this stage, but the physical form (fine sand requiring agglomeration). Recent advances in fine silica agglomeration using organic binders show promising results, with pellets maintaining integrity at furnace temperatures (Manu et al., 2023). Future work should therefore focus on process integration and intensification, such as testing organic acids or closed loop acid regeneration to reduce chemical consumption, and conducting pilot scale trials to validate efficiency and cost parameters under continuous operation.

5 Conclusion

By providing a purified feedstock that meets MG-Si production requirements, this work addresses the foundational step in the multistage PV silicon value chain. The process transforms an abundant, low value sedimentary rock into a strategic industrial material, reducing dependence on imported high purity quartz, and enhancing supply chain resilience for the growing solar energy sector. This study successfully establishes the adaptation and refinement purification techniques for a complex detrital

matrix transforming quartzose sandstone into high purity silica concentrate.

Scientific significance: The study provides the first comprehensive dataset on sandstone beneficiation, delivering key insights into impurity liberation behavior, quantifying the efficiency of each process stage, and offering a mechanistic interpretation of the acid leaching optimization. It establishes that the 250–400 μm fraction and 4 M HCl at 90 °C for 2 h are the optimal parameters for this feedstock.

Industrial significance: The protocol demonstrates a clear technical pathway to convert a low value, locally abundant raw material (Algerian Numidian sandstone) into a high value industrial product (99.28% SiO_2 , 0.02% Fe_2O_3 , 0.02% Al_2O_3) suitable for metallurgical grade silicon production and as a superior feed for further solar grade refining. This contributes directly to supply chain diversification, import substitution, and regional economic development within the growing solar energy sector.

Data availability statement

The original contributions presented in the study are included in the article/supplementary material, further inquiries can be directed to the corresponding author.

Author contributions

HC: Writing – original draft, Writing – review and editing, Methodology, Supervision, Visualization. ZK: Conceptualization, Data curation, Formal Analysis, Writing – original draft, Software. OA: Conceptualization, Data curation, Formal Analysis, Writing – review and editing, Software. DA: Supervision, Writing – review and editing.

Funding

The author(s) declared that financial support was not received for this work and/or its publication.

References

- Abed, M., and Hakem, A. (2017). Ressources Minérales de l'Algérie : Wilaya de Tizi Ouzou. 2nd Edn. Alger, Algérie: Agence du Service Géologique de l'Algérie (ASGA). Unpublished booklet.
- Agence de Service Géologique de l'Algérie (ASGA) (2015). Ressources minérales de l'Algérie des 48 wilayas. 2nd Edn. Ministère de l'industrie et des mines. Unpublished booklet.
- Belousov, V. V., and Ismailov, T. A. (1987). Reserve estimation and mining feasibility of siliceous sandstone deposits, northern Algeria. Unpublished Technical Report. ORGM.
- Bouabdallah, S., Mohamed, B., and Chaib, A. (2015). Removal of iron from sandstone by magnetic separation and leaching: case of El-Aouana deposit (algeria). *Min. Sci.*, 33–44. doi:10.5277/msc152203
- Braga, A. F. B., Moreira, S. P., Zampieri, P. R., Bacchin, J. M. G., and Mei, P. R. (2008). New processes for the production of solar-grade polycrystalline silicon: a review. *Sol. Energy Mater. Sol. Cells* 92 (4), 418–424. doi:10.1016/j.solmat.2007.10.003
- BRGM (2019). Fiche de criticité - Silicium métal. Available online at: <https://www.brgm.fr/sites/default/files/documents/fiche-criticite-silicium-metal.pdf>.
- Chaa, H., Krouri, Z., Akli, O., Allam, D., and Mokaddem, S. (2025). Characterization of Silica in sandstone rocks for advanced energy applications. *Int. J. Energetica* 9 (2), 67–73. doi:10.47238/ijeca.v9i2.259
- Chen, H., Morita, K., Ma, X., Chen, Z., and Wang, Y. (2019). Boron removal for solar-grade silicon production by metallurgical route: a review. *Sol. Energy Mater. Sol. Cells* 203, 110169. doi:10.1016/j.solmat.2019.110169
- Chkotov, A. (1979). Rapport sur les résultats des travaux de recherches effectués en 1976-78 sur les sables quartzeux et grès dans les régions du Nord-Est de l'Algérie.
- Désindes, L. (2005). Silice ultra-pure pour l'électrometallurgie: géologie et caractéristiques physiques et chimiques du minerai quartz. Doctoral dissertation, École Nationale Supérieure des Mines de Paris. HAL Open Science. Available online at: <https://hal.science/tel-00008787>.
- Dvoretiskii, N. V., Anikanova, L. G., Malysheva, Z. G., and Koshel, G. N. (2002). Kinetic parameters of dissolution of Iron(III) oxides of varied thermal and chemical prehistory in hydrochloric acid. *Russ. J. Appl. Chem.* 75, 1207–1210. doi:10.1023/a:1020923919364

Acknowledgements

The authors wish to express their sincere appreciation to the Research Center of Physico-Chemical Analysis (CRAPC), the National School of Marine Sciences and Coastal Management (ENSSMAL), and the Research Center for Studies and Technical Services for the Construction Materials Industry (CETIM) for granting access to their analytical equipment (XRF, XRD, and granulometric analysis). We are deeply grateful to Professor Mezouar Khoudir for his assistance to elaborate this work and to Hamid Zaroub for his essential help on the XRF analysis.

Conflict of interest

The author(s) declared that this work was conducted in the absence of any commercial or financial relationships that could be construed as a potential conflict of interest.

Generative AI statement

The author(s) declared that generative AI was not used in the creation of this manuscript.

Any alternative text (alt text) provided alongside figures in this article has been generated by Frontiers with the support of artificial intelligence and reasonable efforts have been made to ensure accuracy, including review by the authors wherever possible. If you identify any issues, please contact us.

Publisher's note

All claims expressed in this article are solely those of the authors and do not necessarily represent those of their affiliated organizations, or those of the publisher, the editors and the reviewers. Any product that may be evaluated in this article, or claim that may be made by its manufacturer, is not guaranteed or endorsed by the publisher.

- Götze, J., and Möckel, R. (2012). *Quartz: deposits, mineralogy and analytics* (Berlin: Springer).
- Gouski, D., and Ourak, A. (1986). Rapport final sur les résultats des études géologiques expéditives des ressources en matières premières siliceuses du centre Est ALGERIEN. Alger, Algérie: SONAREM. Unpublished report.
- Hadjem, R. (2010). Les principales caractéristiques géologiques, pétrographiques, minéralogiques et géologiques des formations gréseuses du flysch numidien du Nord-est Algérien. Magister thesis. Badji Mokhtar Annaba University. Available online at: <https://biblio.univ-annaba.dz/wp-content/uploads/2014/04/memoire-Hadjem-Riad.pdf>
- Huang, H., Li, J., Li, X., and Zhang, Z. (2013). Iron removal from extremely fine quartz and its kinetics. *Sep. Purif. Technol.* 108, 45–50. doi:10.1016/j.seppur.2013.01.046
- Kefaifi, A., Sahraoui, T., Bobocioiu, E., and Kheloufi, A. (2020). Algerian silica behavior Study at high temperature for carbothermic process. *Silicon* 12, 2861–2867. doi:10.1007/s12633-020-00384-7
- Kheloufi, A., Fathi, M., Rahab, H., Kefaifi, A., Keffous, A., and Medjahed, S. A. (2013). Characterization and quartz enrichment of the hoggar deposit intended for the electrometallurgy. *Chem. Eng. Trans.* 32, 889–894. doi:10.3303/CET1332149
- Manu, K., Mousa, E., Ahmed, H., Elsadek, M., and Wen, Y. (2023). Maximizing the recycling of iron ore pellets fines using innovative organic binders. *Mater. (Basel)* 16 (10), 3888. doi:10.3390/ma16103888
- Nouioua, A., and Barkat, D. (2017). Liquid-Liquid extraction of iron (III) from Ouenza iron ore leach liquor by Tri Butyl phosphate. *J. Fundam. Appl. Sci.* 9 (3), 1473. doi:10.4314/jfas.v9i3.14
- Pan, X., Li, S., Li, Y., Guo, P., Zhao, X., and Cai, Y. (2022). Resource, characteristic, purification and application of quartz: a review. *Miner. Eng.* 183, 107600. doi:10.1016/j.mineng.2022.107600
- Schei, A., Tuset, J., and Tveit, H. (1998). *Production of high silicon alloys*. Trondheim: TAPIR.
- Vatalis, K. I., Charalambides, G., and Benetis, N. P. (2015). Market of high purity quartz innovative applications. *Procedia Economics and Finance* 24, 734–742. doi:10.1016/S2212-5671(15)00688-7
- Wang, W., Cong, J., Deng, J., Weng, X., Lin, Y., Huang, Y., et al. (2018). Developing effective separation of feldspar and quartz while recycling tailwater by HF pretreatment. *Minerals* 8 (4), 149. doi:10.3390/min8040149
- Wang, C., Li, G., Lin, X., Gao, T., Pang, Z., Sun, C., et al. (2025). Research on the purification technology of quartz from a mining area in Jiangxi by acid leaching. *Minerals* 15 (11), 1200. doi:10.3390/min15111200
- Wills, B. A., and Finch, J. A. (2015). *Wills' mineral processing technology: an introduction to the practical aspects of ore treatment and mineral recovery*. 8th ed. Oxford: Butterworth-Heinemann.
- Xie, Y., Li, S., Pan, X., Li, Y., and Zhang, A. (2023). Recent advances in the marketing, impurity characterization and purification of quartz. *Minerals and Mineral Materials* 2 (1), 16. doi:10.20517/mmm.2023.17
- Yu, D., Ma, Y., Wang, S., Ma, C., and Wei, F. (2025). Mineralogy and preparation of high-purity quartz: a case Study from pegmatite in the Eastern sector of the north qinling orogenic Belt. *Minerals* 15 (8), 788. doi:10.3390/min15080788
- Zhang, Z., Li, J., Li, X., Huang, H., Zhou, L., and Xiong, T. (2012). High efficiency iron removal from Quartz sand using phosphoric acid. *International Journal of Mineral Processing* 114–117, 30–34. doi:10.1016/j.minpro.2012.09.001
- Zhang, T., Huang, Y., Sun, H., Tang, Y., and Peng, T. (2025). Waste quartz crucible crystallization-induced purification to prepare high-purity cristobalite sand. *Minerals* 15 (11), 1184. doi:10.3390/min15111184